

Article

Influence of Boron and Nitrogen on the Machinability, Polishability and Wear of Martensitic Stainless Steels

Marko Sedlaček ^{1,*} , Barbara Šetina Batič ¹ , Vesna Žepič Bogataj ² and Jaka Burja ¹ 

¹ Institute of Metals and Technology, University of Ljubljana, Lepi Pot 11, 1000 Ljubljana, Slovenia; barbara.setina@imt.si (B.Š.B.); jaka.burja@imt.si (J.B.)

² Slovenian Tool and Die Development Centre, TECOS, 3000 Celje, Slovenia; vesna.zepic.bogataj@tecos.si

* Correspondence: marko.sedlacek@imt.si; Tel.: +386-1-4701-931

Abstract: The utilization and advancement of a wide variety of polymer materials have led to the development of corresponding plastic injection mould steels. This study aimed to enhance the properties of the commercially available steel EN X33CrS16 (1.2085), specifically designed for corrosion-resistant mould bases. To achieve this, the impact of the addition of boron and nitrogen into the commercially available steel grade was examined, focusing on their effects on polishability, workability, and wear resistance. The analysis revealed a martensitic microstructure with moderate segregation in all investigated samples. The steel modification had no discernible impact on hardness, which remained relatively constant. However, the addition of boron and nitrogen significantly reduced polishing time, with boron exhibiting a more pronounced effect compared to nitrogen. Moreover, the inclusion of boron in the alloy resulted in an impressive 40% decrease in the wear rate, while the wear rate of the other investigated alloys remained relatively unchanged.

Keywords: martensitic stainless steel; boron; nitrogen; wear; machinability; polishability



Citation: Sedlaček, M.; Šetina Batič, B.; Žepič Bogataj, V.; Burja, J.

Influence of Boron and Nitrogen on the Machinability, Polishability and Wear of Martensitic Stainless Steels.

Metals **2023**, *13*, 1759. <https://doi.org/10.3390/met13101759>

Academic Editor: Antonio Mateo

Received: 29 September 2023

Revised: 12 October 2023

Accepted: 14 October 2023

Published: 17 October 2023



Copyright: © 2023 by the authors. Licensee MDPI, Basel, Switzerland. This article is an open access article distributed under the terms and conditions of the Creative Commons Attribution (CC BY) license (<https://creativecommons.org/licenses/by/4.0/>).

1. Introduction

The utilization and development of a wide array of polymer-based materials, including composites, have driven the concurrent progress of plastic injection mould steels. To enhance the mechanical properties of polymer matrices, reinforcements in the form of fibers or whiskers are introduced into the material. However, these reinforcements due to their abrasive nature, can affect and accelerate the wear of the moulds. Notably, significant surface deterioration is often observed on the mould mouldrunners and cavity gates, while the core and cavity surfaces can also suffer critical wear damage [1]. The industrial sector that employs polymers places considerable emphasis on the surface condition of moulds, considering both aesthetics and functionality. As damage to the steel surface translates to the finished product's surface, particular attention is given to acceptable levels of defects and imperfections that may appear on injection moulded plastic parts. Consequently, extensive advancements have been made in plastic mould steel series, encompassing carbon steel, carburized plastic mould steel, aging-hardening plastic mould steel, corrosion-resistant plastic mould steel, free-machining plastic mould steel, through-hardening plastic mould steel, maraging plastic mould steel, and mirror-polishing plastic mould steel, among others [2].

Most steels used in the polymer injection moulding process consist of a martensitic matrix with varying types and distributions of carbides within the structure. Their optimization is achieved through heat treatment. Alternatively, the implementation of hard protective coatings on the surface of tools and moulds also serves as an effective solution [1,3,4].

On the other hand, steel properties, such as machinability and polishability, are closely linked to its chemical composition and microstructure. Segregations within the

microstructure and the presence of different carbides have a direct impact on surface finish and wear resistance. Modifying the microstructure can be achieved by altering the steel's chemical composition, which involves the addition of different elements to manipulate its properties. It was shown [5] that copper effectively enhances the corrosion resistance of pre-hardened mould steel and reduces the cutting force of the steel while improving surface finish [6]. Additionally, it was shown [6] that addition of sulfur reduces the cutting force of P20 plastic mould steels, but decreases polishing performance.

While sulfur is typically considered an impurity, it is intentionally added to certain steels. Steels for the production of frames for plastic moulds frequently need to exhibit resistance to corrosion while at the same time requiring large amounts of machining. Machinability as a crucial property can be enhanced by the addition of sulfur, resulting in the formation of favorable sulfides, which in turn can deteriorate mechanical properties and corrosion resistance [7]. The addition of sulfur is known to enhance machinability but can reduce transverse ductility and notched impact toughness. During solidification, sulfur combines with manganese to form manganese sulfide (MnS) non-metallic inclusions. Manganese sulfides play a vital role in improving machinability [4,8,9]. When machining, MnS acts as a lubricant, reducing friction and extending tool life while yielding a superior surface finish. Additionally, MnS promotes the formation of short machine turnings, which enhances machinability by reducing tool wear, improving chip control, enhancing surface finish, and minimizing the risk of workpiece damage. In addition to its impact on machinability, sulfur has minimal effects on the longitudinal mechanical properties of steel. Free cutting steels specifically have sulfur added to enhance machinability, with typical contents above 0.35%.

Boron is another element that is commonly added to steels to modify their properties. Its most significant effect is the pronounced improvement of the hardenability of medium carbon steels, albeit at the expense of forging quality. Hardenability refers to the property that determines the depth and distribution of hardness achieved through quenching. Even a small amount of boron (ranging from 0.0005% to 0.003%) can produce the same increase in hardenability as other elements that are required in larger quantities.

The use of boron nitride (BN) also demonstrated enhanced machinability in austenitic stainless steels [9] and heat-treatable steels [10,11]. Chen et al. showed the potential benefits of using both manganese sulfides (MnS) and boron nitride (BN) simultaneously to improve machinability [12]. However, it should be noted that high boron contents can lead to hot cracking and embrittlement, particularly in carbon steels, due to the formation of low-melting ternary eutectic [13]. Consequently, the boron content must be carefully controlled and aligned with the carbon content. However, the high contents of chromium in stainless steels prevents the formation of the low temperature ternary eutectic. Titanium and aluminum are often added alongside boron because boron has a strong affinity for oxygen and nitrogen. Boron oxides and nitrides do not contribute to increased hardenability.

Increasing the nitrogen content in steels has several effects on their properties. It leads to increased hardness and yield strength while reducing tensile elongation [14]. Steels containing nitrogen also exhibit improved corrosion resistance [15]. High-nitrogen stainless steels demonstrate higher corrosion-erosion resistance compared to conventional AISI 420 stainless steel, which can be attributed to the beneficial effect of nitrogen in solid solution within the martensite structure [16]. Nitrogen is more readily dissolved during austenitization compared to carbon, resulting in a lower carbon-to-nitrogen ratio at the hardening temperature. This, in turn, is likely to enhance the corrosion resistance of martensite after quenching [17]. The solubility of nitrogen in the steel matrix varies depending on the chemical composition, and elements such as chromium (Cr) and manganese (Mn) increase nitrogen solubility [18]. Although there are new technologies such as 3D-printed moulds [19] and the use of alternative materials [20], moulds made of conventional materials such as steel or aluminum remain in use and it is necessary to adapt their properties to the injection moulding of new materials.

The aim of this study was to enhance the properties of the commercially available steel EN X33CrS16 (1.2085), specifically designed for corrosion-resistant mould bases. The focus was on modifying its microstructure to maintain the same hardness while improving machinability, polishability, and wear resistance. To achieve this, the effects of adding boron and nitrogen to the commercially available steel grade were investigated, with a particular emphasis on their impact on polishability, workability, and wear resistance.

2. Materials and Methods

2.1. Material and Heat Treatment

This study focused on the utilization of martensitic stainless steel 1.2085, which is specifically designed for corrosion-resistant mould bases, tool sets, and moulds used in applications involving corrosive plastics like PVC. The steel composition typically consists of approximately 0.3% carbon (C) and 16% chromium (Cr), providing it with favorable mechanical strength and corrosion resistance. To improve machinability, the steel also contains sulfur, although this compromises polishability and reduces corrosion resistance.

The experimental part in this work involved testing the industrial-grade material, a re-melted material, and modified materials with increased boron or nitrogen contents. An induction melting furnace was utilized to produce laboratory-scale 8 kg ingots. To prevent oxidation, argon gas was blown onto the melt surface during the melting process, and either ferroboration or ferrochromium nitride (4% N) was added. The resulting ingots, measuring 60 mm × 60 mm, were heated to 1200 °C and hot rolled into 20 mm strips.

Table 1 presents the chemical composition of the investigated steels. The industrial batch was labeled as MSS-ind, and to examine the influence of higher remelting and solidification rates on properties, the industrial batch was remelted and denoted as MSS-0. The chemical composition of the industrial and remelted batches remained the same. Samples that had boron added (0.032 wt%) were labeled as MSS-B, while samples with added nitrogen (0.17 wt% N) were labeled as MSS-N. Values of added boron and nitrogen were chosen according to thermodynamic calculations where B content was chosen as point of BN precipitation at 1600 °C, while N content was chosen as the upper limit of N solubility at 1400 °C. The microstructure of all samples was observed to be martensitic with some presence of delta ferrite, with detailed explanations provided later in the text.

Table 1. Chemical composition of investigated steel (wt%).

Specimen	C	Si	Mn	Cr	Ni	Mo	N	B	S
MSS-ind	0.275	0.26	1.35	15	0.69	0.09	0.072	0.0008	0.076
MSS-0	0.274	0.27	1.37	15	0.69	0.09	0.073	0.0009	0.075
MSS-B	0.274	0.35	1.36	14.9	0.69	0.08	0.066	0.032	0.074
MSS-N	0.25	0.22	1.27	16.5	0.69	0.08	0.169	0.0005	0.074

After hot rolling, the strips were cut into smaller 200 mm plates. The plates were annealed at 1030 °C for 30 min and quenched in oil and then tempered in two steps at 620 °C for 2 h and 630 °C for 2 h, to achieve a hardness of around 300 HB.

2.2. Characterization

All samples were metallographically prepared by grinding with SiC papers, followed by polishing with 3 to 1 µm diamond suspension, and finally etching with 5 vol% Nital for light optical microscopy (Olympus DP70 LOM, (Olympus, Tokyo, Japan). Microstructure and wear tracks were analyzed at different magnifications using scanning electron microscopy (ZEISS CrossBeam 550, Zeiss, Oberkochen, Germany).

2.3. Hardness

Influence of different chemical composition on hardness was measured according to Brinell hardness. Hardness on each type of sample was measured using Inovatest NEXUS 7500 test machine (INNOVATEST Europe BV, Maastricht, Netherlands) according to ISO 6506-1:2014 standard [21].

2.4. Polishability

Polishability was investigated using an in-house method where the time to reach the high gloss polished surface is measured and the difficulty of polishing is rated. A high gloss polished surface is defined as when the surface roughness is $S_a \leq 0.05 \mu\text{m}$. Difficulty of polishing is rated from 1 to 10, where 1 is difficult and 10 is easier to polish. Special observations or peculiarities are noted.

2.5. Chip Forming

Chip formation was investigated using a CNC milling machine (HAAS, Oxnard, CA, USA). A new carbide end mill 5RX15X100L (JJ Tools, Seoul, South Korea) was used for each sample. The same parameters according to the manufacturer's specifications (8000 RPM, FEED 1100 mm/min and depth of cut 0.3 mm) were used on all samples. During the machining, chips were collected and analyzed under the optical microscope. Chip forms were determined according to the ISO 3685-1993 (E) standard [22]. Cutting edges on the end mills were also analyzed after the tests.

2.6. Tribological Testing

To assess the wear properties of the investigated steels and eliminate the influence of other factors, a model test employing reciprocating sliding was conducted. Model wear tests were performed in order to eliminate other potential influences on wear results. The test parameters and contact materials were selected so that the predominant wear mechanism was abrasion, as in real contact. The wear resistance of the materials was evaluated using a ball-on-flat contact configuration (Figure 1). To concentrate wear on the steel samples, a much harder Al_2O_3 ball was used as the counter body. The chosen ball had a diameter of 32 mm and a hardness ranging from 1250 to 1700 HV.

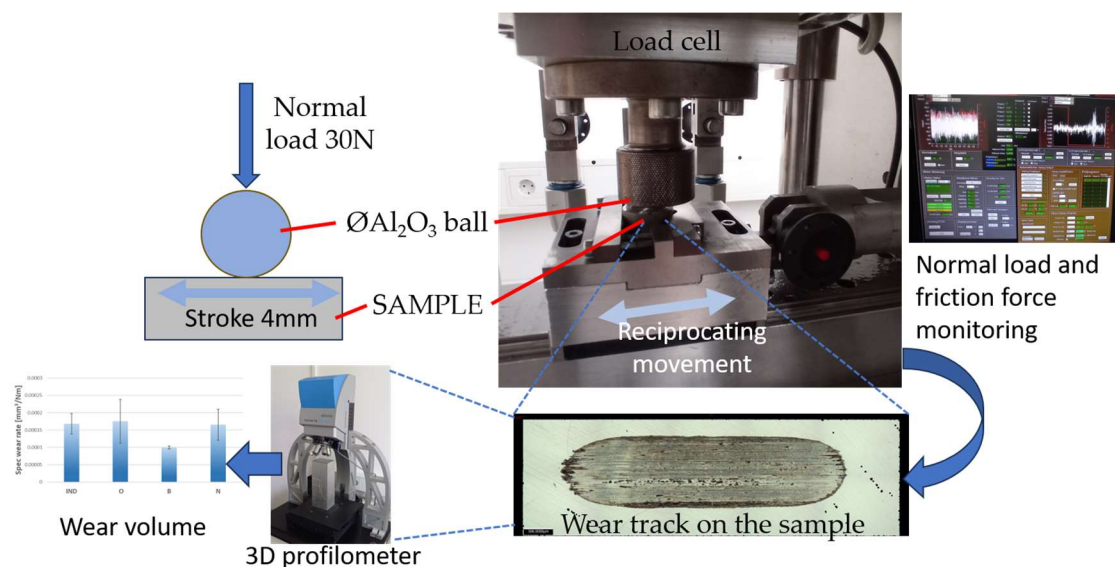


Figure 1. Schematic presentation of tribological experimental setup.

To minimize the impact of surface topography, all samples were mirror polished ($S_a = 0.05 \mu\text{m}$) prior to testing.

In order to achieve measurable wear within a relatively short testing duration, the test parameters were optimized. A normal load of 30 N, corresponding to a nominal Hertzian contact pressure of 0.6 GPa, was applied. The reciprocating sliding frequency was set at 45 Hz, corresponding to a sliding speed of 0.12 m/s. The sliding distance was limited to 100 m. To ensure repeatability, each material was tested in at least three repetitions. The coefficient of friction was recorded during the tests. After the completion of the tests, wear volumes were measured using a 3D profilometer Alicona Infinite Focus G4 (Bruker Alicona, Raaba-Grambach, Austria). Optical and scanning electron microscopes were employed to analyze the wear tracks. The specific wear rate was calculated for all wear measurements. The specific wear rate is defined as the wear volume (mm^3) divided by the product of the normal load (N) and the sliding distance (m).

3. Results and Discussion

3.1. Microstructure

Light microscopy revealed that the industrial batch (Figure 2a) results in a martensitic microstructure with moderate segregation, with primary and secondary carbides on the MnS inclusions. A large amount of sulfide inclusion can be seen which is elongated and large (Figure 2a). The MSS-ind batch underwent a larger degree of deformation and consequently the MnS inclusions are longer and that is why they appear larger in the metallographic figures due to the etching effect. In the re-melted steel moderate segregation can be seen with a large amount of small round sulfide inclusions. Addition of boron results in moderate segregation. Primary, and secondary carbides on the MnS inclusions can be observed. The non-metallic inclusions are numerous and small (below $5 \mu\text{m}$) with medium-sized round sulfides. Addition of nitrogen results (Figure 2d) in a very martensitic microstructure with heavy segregations and a large number of inclusions which are small with medium-sized round sulfides.

SEM/EDS analysis of non-metallic inclusions (Figure 3d) revealed that the most numerous are MnS inclusions and the largest number can be found in the MSS-ind batch and the lowest in the boron batch MSS-B (Figure 3b). Most of the MnS inclusions correspond to a size of around 10 microns (Figure 3c). In the case of boron batch MSS-B, nucleation of boron nitrides (BN) on aluminate non-metallic inclusions was confirmed (Figure 3a). An area of $10 \text{ mm} \times 30 \text{ mm}$ was analyzed for each sample. Laboratory samples had a higher solidification rate that partly impaired the deformation of large inclusions.

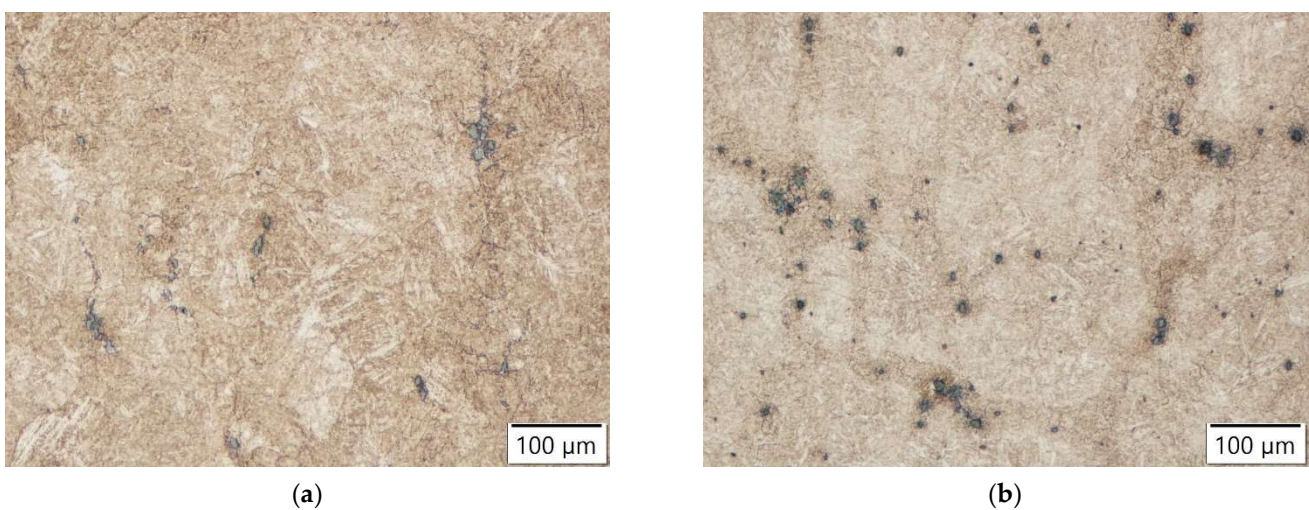


Figure 2. Cont.

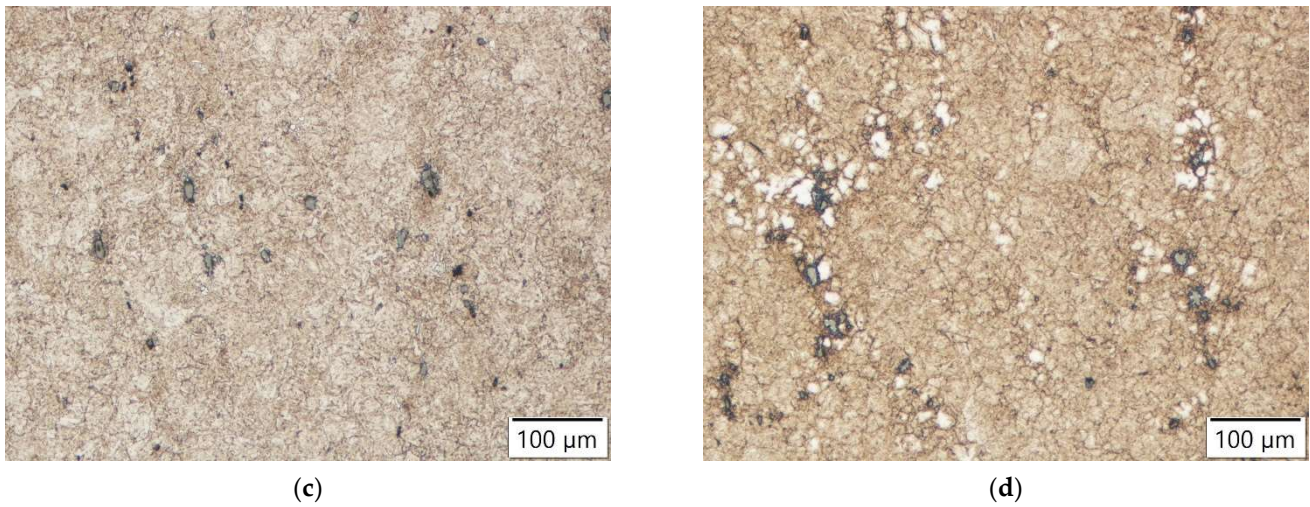


Figure 2. Light microscopy of microstructures on: (a) MSS-ind, (b) MSS-0, (c) MSS-B, and (d) MSS-N.

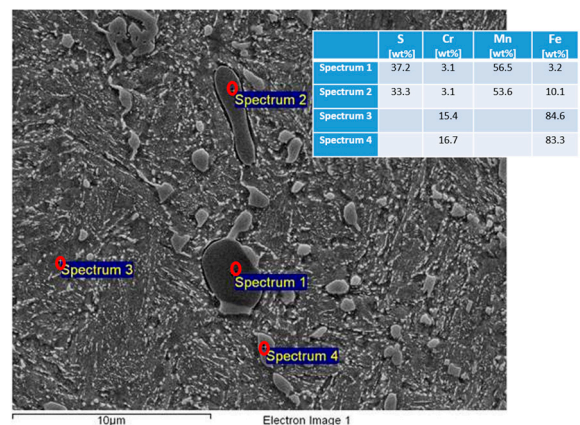
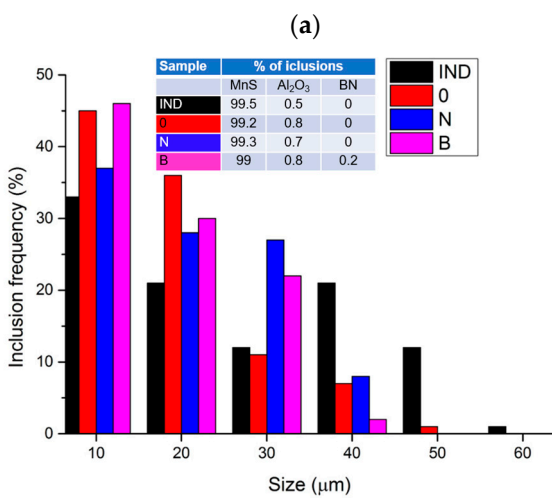
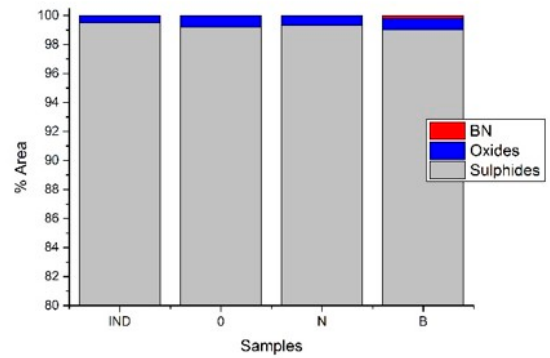
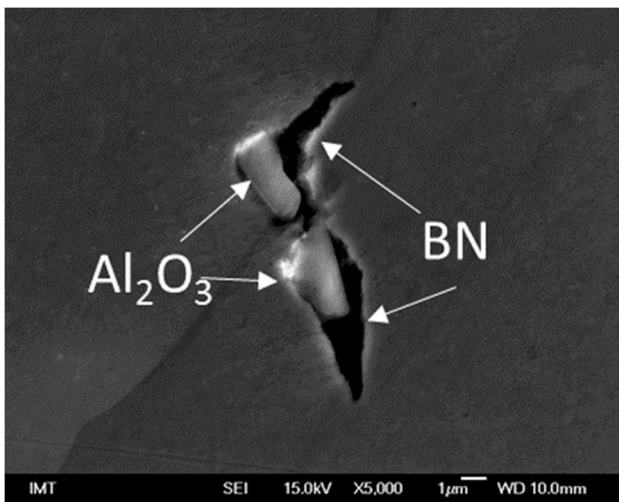


Figure 3. (a) Boron nitride nucleated on aluminate non-metallic inclusions, (b) area occupied by non-metallic inclusions, (c) non-metallic inclusion size distribution, (d) EDS point analysis of MSS-ind.

Findings suggest that the addition of boron and nitrogen can influence the microstructure and presence of non-metallic inclusions in the steel. Boron addition appears to reduce the size and number of inclusions, whereas nitrogen addition, may introduce challenges due to heavy segregations and larger inclusions.

3.2. Hardness

Figure 4 illustrates the Brinell hardness results, demonstrating that the modifications made to the steel resulted in minimal changes in hardness. The remelting process and the addition of boron showed a slight negative impact on hardness, leading to a reduction of approximately 2%. Conversely, the addition of nitrogen led to a slight increase in hardness of around 1.7%.

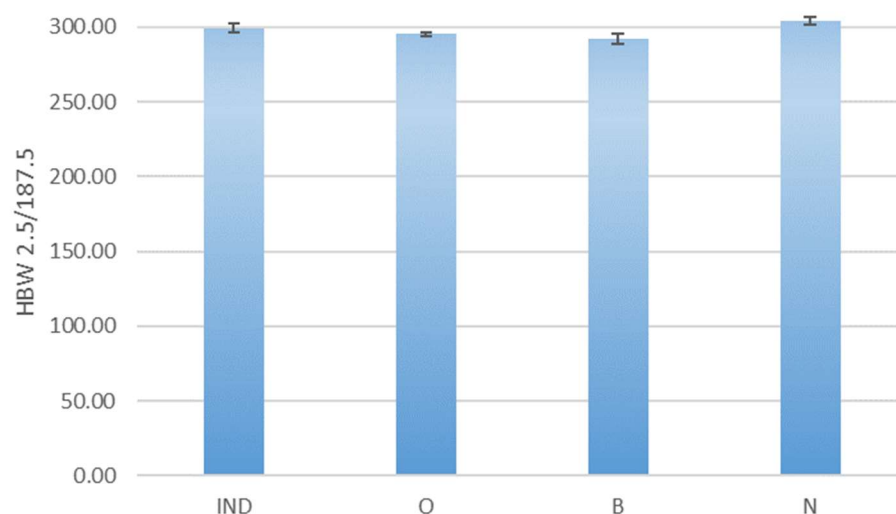


Figure 4. Hardness of investigated samples.

These differences in hardness, however, are quite small, indicating the reliability and consistency of the heat treatment process. They are below 3% and can be considered negligible in practical terms. It is worth noting that segregations in the microstructure can contribute to higher hardness. In the case of the MSS-N sample, which exhibited more pronounced segregations and a higher nitrogen content (a good matrix hardener), the slightly higher hardness was expected.

In general, boron is known to enhance hardness by improving hardenability. However, in this particular case, where the microstructure is already fully hardened, the addition of boron is not expected to significantly affect the hardness in the same manner.

Overall, the observed changes in hardness are minimal and do not significantly impact the properties of the steel.

3.3. Polishability

On all investigated samples, the measured roughness was less than $Sa \leq 0.05 \mu\text{m}$ so the criterium for a highly glossy, polished surface was met. In Table 2 where the time and difficulty of polishing are presented, it can be seen that the industrial batch is hardly polishable as the time and difficulty are the worst among all investigated samples. Remelting of material resulted in a 33% shorter polishing time. In general addition of boron and nitrogen to steel improves polishability by enhancing hardenability, promoting a fine grain structure, and maintaining or improving strength and hardness properties. These factors collectively contribute to achieving a smoother and more polished surface in the steel.

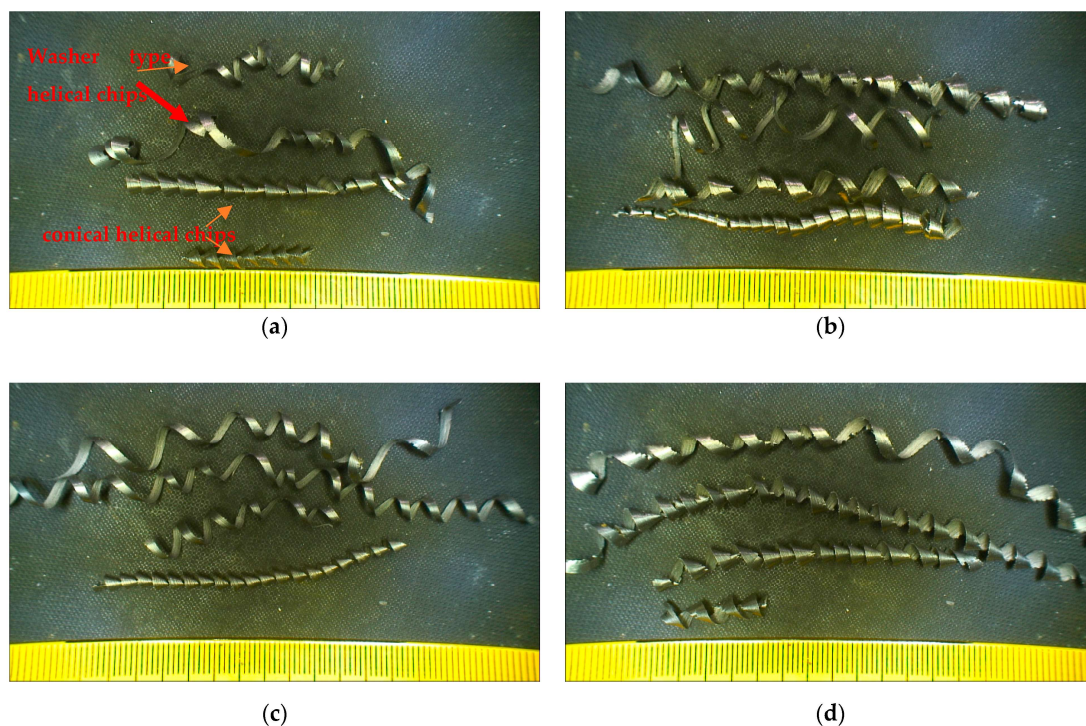
Table 2. Time and difficulty of polishing for investigated samples.

Specimen	Time of Polishing [min]	Difficulty of Polishing	Remarks
MSS-IND	210	2	fog at edge
MSS-0	140	5	/
MSS-B	135	7	crack in material
MSS-N	150	5	/

Polishability in plastic moulds is crucial for achieving high-quality, visually appealing, and consistent moulded parts. In addition to that, polishability directly impacts the surface finish of the moulded plastic parts; it also impacts the production efficiency and longevity of the mould, making it an essential consideration in industries where product appearance and quality are paramount.

3.4. Chip Forming

Figure 5 displays the typical chips obtained during the milling process for the investigated samples. Across all samples, conical helical chips are predominantly observed. There are also instances of washer-type helical chips, although they are less common.

**Figure 5.** Representative chips obtained by milling: (a) MSS-ind, (b) MSS-0, (c) MSS-B, (d) MSS-N.

Notably, the MSS-ind sample produces the shortest chips, while the MSS-N sample generates the longest chips. It can be concluded that the formation of smaller round sulfide inclusions obtained by remelting or addition of boron or nitrogen, leads to more controlled chip formation in the shape of longer conical helical chips. Continuous chips, characterized by uninterrupted formation, are generally preferred due to their positive impact on surface finish, reducing friction, extending tool life, having lower power consumption, and overall improving machining performance.

Upon analysis of the cutting edges on the end mills, no signs of wear were detected. This lack of wear can be attributed to the relatively short duration of the machining process. Since wear typically occurs over longer periods of continuous use, the absence of wear on

the cutting edges suggests that the machining time was not extensive enough to induce noticeable wear performance on the end mills.

3.5. Wear Properties

The results of the abrasive wear tests are presented in Figure 6, where the specific wear rate for the investigated samples is displayed.

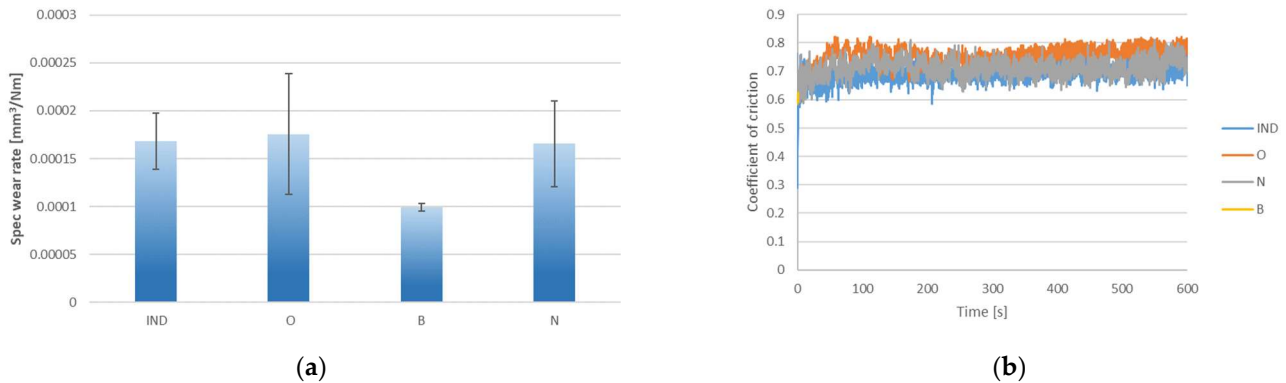


Figure 6. (a) Specific wear rate and (b) coefficient of friction of investigated samples.

The remelting of material MSS (MSS-0) did not have a significant effect on the wear rate, with only a slight deterioration of 4% observed.

In contrast, the addition of boron (MSS-B) had a beneficial effect, resulting in a notable reduction of 41% in the wear rate. This improvement can be attributed to the formation of boron nitrides and the shortening of manganese sulfide (MnS) inclusions in the microstructure.

The effect of nitrogen (MSS-N) on the wear rate was found to be negligible when compared to the industrial batch (MSS-ind).

The coefficient of friction was relatively consistent across all samples, with values around 0.75 ± 0.04 (Figure 6b).

3.6. Wear Tracks Analysis

The analysis of the wear track in the investigated materials confirmed that the main wear mechanism observed was abrasion (Figure 7). This can be attributed to the presence of a much harder counterbody material, in this case, Al_2O_3 . The abrasive nature of the counterbody caused the material to be removed from the wear surface through mechanical actions such as scratching and plowing.

In addition to the observed adhesion in the wear track, traces of adhesion of the removed material were observed in some parts of the wear track, as shown in Figure 7. Analysis using EDS mapping confirmed that the adhered material was composed of the removed material from the samples. This suggests that during the wear process, the material from the investigated samples underwent localized melting and welding with the counterbody, leading to the transfer and deposition of the removed material onto the wear track. Furthermore, traces of transfer of Al_2O_3 from the counterbody material were also observed, as depicted in Figure 8. This indicates that during the abrasive wear process, some particles of the harder Al_2O_3 counterbody were detached and transferred onto the wear surface of the investigated samples. The transfer of Al_2O_3 particles can further contribute to the abrasive wear process, as these particles act as additional abrasive agents, causing further material removal from the wear surface. The most traces of adhesion were observed on the samples MSS-0 and MSS-N. This can be attributed to the specific properties of these materials, such as their chemical composition and microstructure. The higher adhesion observed in these samples may be linked to their composition and the presence of certain elements, which could promote material sticking and welding under the test conditions.

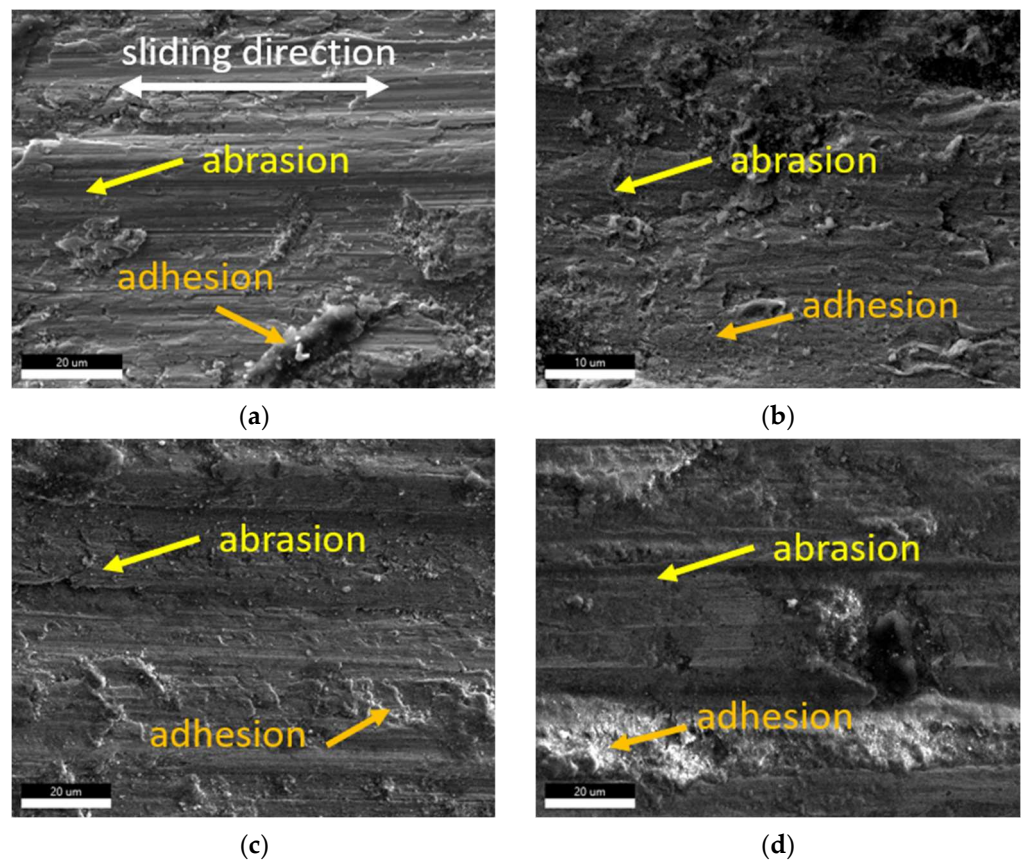


Figure 7. Wear track at 1000× magnification on sample: (a) MSS-ind, (b) MSS-0, (c) MSS-B, (d) MSS-N.

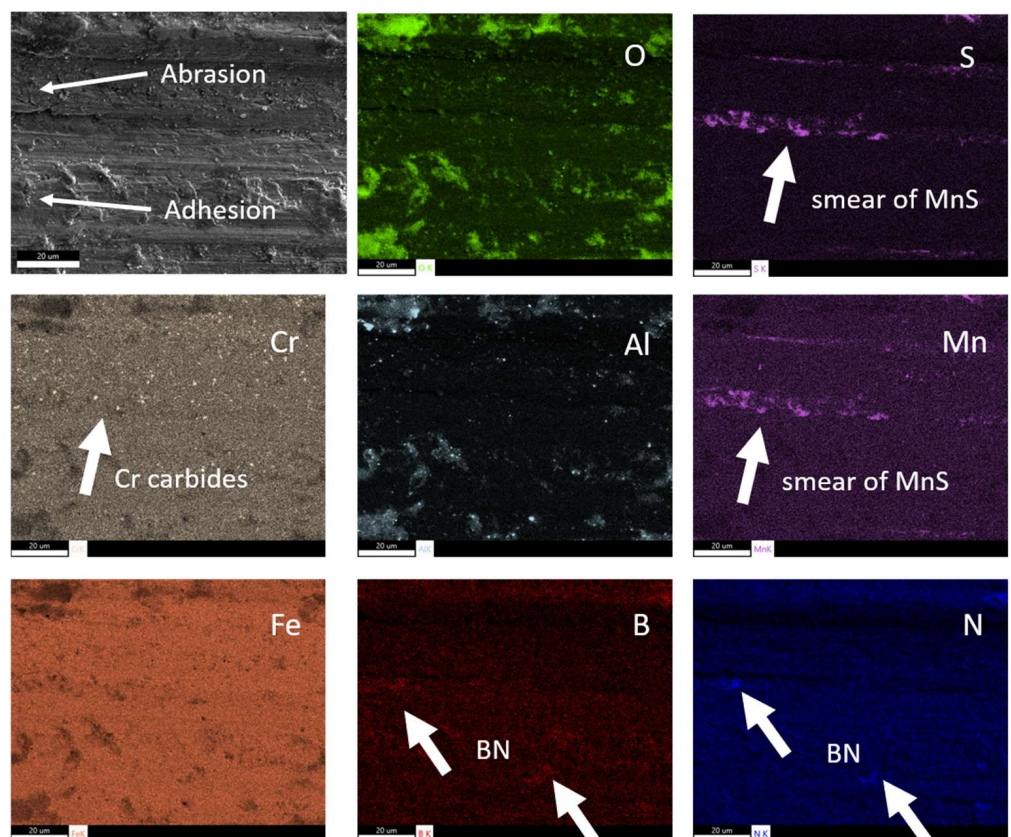


Figure 8. Mapping of wear track on MSS-B at 1000× magnification.

The detailed analysis of the wear track using EDS mapping revealed the presence of clusters of MnS in all investigated alloys. Figure 9 illustrates an untacked surface of the sample MSS-B, where the MnS clusters can be observed. These clusters play a significant role in the wear process, as shown in Figure 8. During wear, the MnS clusters separate and act as lubricants, reducing friction and contributing to less wear. This lubricating effect is beneficial for all investigated materials.

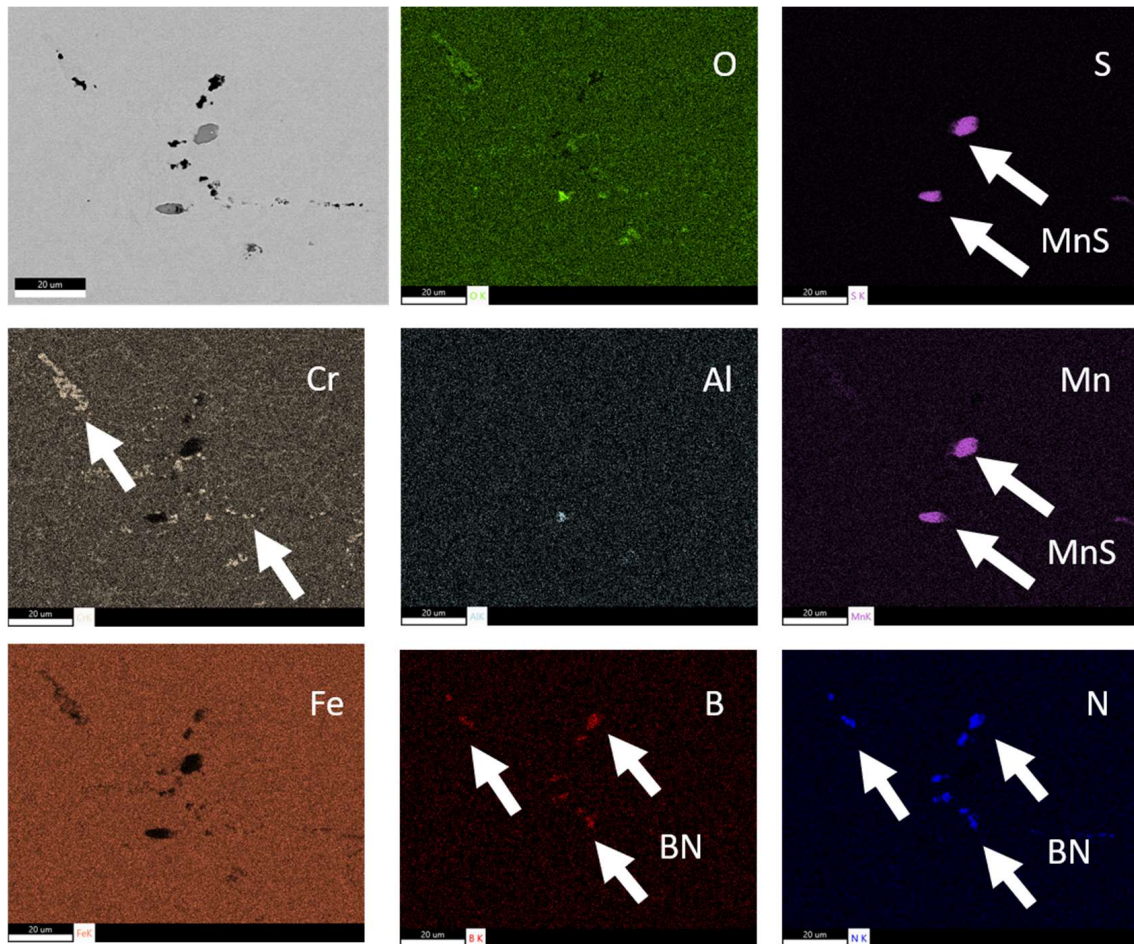


Figure 9. Mapping of polished surface of MSS-B at 1000 \times magnification.

Additionally, globular Cr carbides were observed in all investigated samples, and they remained untacked after the tribological tests. These Cr carbides also contribute to reducing wear by providing a protection of the matrix as they reduce direct contact between the surfaces. Moreover, in the case of the MSS-B sample, boron nitride particles were also observed, and they remained intact in the matrix even after the wear tests. The presence of hard boron nitride particles can contribute to enhancing the wear resistance of the investigated materials; being hard and resistant to wear, they can act as reinforcement within the material matrix and provide additional support against abrasive wear. Their presence can help reduce the direct contact between surfaces, minimize friction, and prevent material loss due to abrasive action.

The combination of the lubricating effect of MnS clusters and the reinforcement provided by hard BN particles can synergistically improve the wear resistance of the alloys. By reducing friction and protecting the material surface, these particles can contribute to prolonging tool life, reducing wear rates, and improving the overall performance of the materials in abrasive wear conditions.

4. Conclusions

Based on the provided information, the following conclusions can be drawn.

Microstructure: All investigated samples exhibited a martensitic microstructure with moderate segregation.

Hardness: The modification of the steel did not have a significant effect on hardness. The hardness values remained relatively constant within the range of 297 ± 5 HBW for all samples.

Polishing Time: Remelting of the material resulted in a 33% reduction in polishing time. Additionally, the addition of boron and nitrogen further decreased the polishing time, with boron being more effective than nitrogen.

Chip Formation: The material MSS-ind exhibited the shortest chip formation, while the addition of nitrogen (MSS-N) resulted in the longest chips.

Wear Rate: The addition of boron to the alloy significantly reduced the wear rate by almost 40% compared to other investigated alloys. This improvement can be attributed to the formation of boron nitrides, which contribute to enhanced wear resistance. Traces of MnS acting as a lubricant were observed in all investigated alloys, further aiding in reducing wear.

In summary, the modifications made to the steel, particularly the addition of boron, showed positive effects on polishing time and wear resistance. The presence of boron nitrides and the lubricating properties of MnS contributed to the improved performance of the alloys in terms of wear characteristics.

Author Contributions: Conceptualization, M.S., V.Ž.B. and J.B.; methodology, V.Ž.B. and J.B.; validation, M.S., B.Š.B., V.Ž.B. and J.B.; formal analysis, M.S. and B.Š.B.; investigation, M.S. and J.B. writing—original draft preparation, M.S.; writing—review and editing B.Š.B., V.Ž.B. and J.B. All authors have read and agreed to the published version of the manuscript.

Funding: This research was funded by the Slovenian Research and Innovation Agency, research core funding No. P2-0050.

Data Availability Statement: The data presented in this study are available on request from the corresponding author. The data are not publicly available due to restrictions regarding an on-going funded research.

Conflicts of Interest: The authors declare no conflict of interest. The funders had no role in the design of the study; in the collection, analyses, or interpretation of data; in the writing of the manuscript, or in the decision to publish the results.

References

1. Bergstrom, J.; Thuvander, F.; Devos, P.; Boher, C. Wear of Die Materials in Full Scale Plastic Injection Moulding of Glass Fibre Reinforced Polycarbonate. *Wear* **2001**, *251*, 1511–1521. [[CrossRef](#)]
2. Gehricke, B.; Schruoff, I. Trend in plastic mould steel applications. In *Tool Steels in the Next Century, Proceedings of the 5th International Conference on Tooling, Leoben, Austria, 29 September–1 October 1999*; Jeglitsch, F., Ebner, R., Leitner, H., Eds.; University of Leoben: Leoben, Austria, 1999; pp. 83–90.
3. Bienk, E.J.; Mikkelsen, N.J. Application of Advanced Surface Treatment Technologies in the Modern Plastics Moulding Industry. *Wear* **1997**, *207*, 6–9. [[CrossRef](#)]
4. Shin, J.H.; Park, J.H. Formation Mechanism of Oxide-Sulfide Complex Inclusions in High-Sulfur-Containing Steel Melts. *Metall. Mater. Trans. B* **2018**, *49*, 311–324. [[CrossRef](#)]
5. Chen, X.; Li, J.; Li, Z.; Li, J.; Wu, X. Effects of a Cu addition on the corrosion resistance of low-alloy pre-hardened plastic mold steel. *Mater. Tehnol.* **2022**, *56*, 381–388. [[CrossRef](#)]
6. Wang, Y.; Chen, X.; Zuo, P.; Wu, X. Influence of Copper and Sulfur on the Cutting Performance of P20-type Plastic Mold Steel. *Cailiao Daobao/Mater. Rep.* **2022**, *36*, 21030076-7. [[CrossRef](#)]
7. Niederhofer, P.; Henke, L.; Frie, D.; Neuenfeldt, M.; Zanger, F. Stainless Steels for Plastic Mold Frames Featuring Enhanced Machinability. *Steel Res. Int.* **2023**, *94*, 2200754. [[CrossRef](#)]
8. Jiang, B.; Wu, M.; Sun, H.; Wang, Z.; Zhao, Z.; Liu, Y. Prediction Model of Austenite Growth and the Role of MnS Inclusions in Non-Quenched and Tempered Steel. *Met. Mater. Int.* **2018**, *24*, 15–22. [[CrossRef](#)]
9. Emura, S.; Kawajiri, M.; Min, X.; Yamamoto, S.; Sakuraya, K.; Tsuzaki, K. Machinability Improvement and Its Mechanism in SUS304 Austenitic Stainless Steel by H-BN Addition. *Tetsu-to-Hagane* **2012**, *98*, 358–367. [[CrossRef](#)]

10. Wang, Y.-N.; Bao, Y.-P.; Wang, M.; Zhang, L.-C. Precipitation and Control of BN Inclusions in 42CrMo Steel and Their Effect on Machinability. *Int. J. Miner. Metall. Mater.* **2013**, *20*, 842–849. [[CrossRef](#)]
11. Chen, Y.-N.; Bao, Y.-P.; Wang, M.; Cai, X.-F.; Wang, L.-J.; Zhao, L.-H. Basic Research on Mechanism of BN Inclusion in Improving the Machinability of Steel. *Rev. Metal.* **2014**, *50*, e028. [[CrossRef](#)]
12. Chen, Y.-N.; Bao, Y.-P.; Wang, M.; Cai, X.-F.; Wang, L.-J.; Zhao, L.-H. Superior Machinability of Steel Enhanced with BN and MnS Particles. *Int. J. Miner. Metall. Mater.* **2016**, *23*, 276–282. [[CrossRef](#)]
13. Ohtani, H.; Hasebe, M.; Ishida, K.; Nishizawa, T. Calculation of Fe-C-B Ternary Phase Diagram. *Trans. Iron Steel Inst. Jpn.* **1988**, *28*, 1043–1050. [[CrossRef](#)]
14. Scott, F.W. Effect of Nitrogen on Steel. *Ind. Eng. Chem.* **1931**, *23*, 1036–1051. [[CrossRef](#)]
15. Horovitz, M.B.; Neto, F.B.; Garbogini, A.; Tschiptschin, A.P. High Nitrogen Steels. Nitrogen Bearing Martensitic Stainless Steels: Microstructure and Properties. *ISIJ Int.* **1996**, *36*, 840–845. [[CrossRef](#)]
16. Toro, A.; Misiólek, W.Z.; Tschiptschin, A.P. Correlations between Microstructure and Surface Properties in a High Nitrogen Martensitic Stainless Steel. *Acta Mater.* **2003**, *51*, 3363–3374. [[CrossRef](#)]
17. Krasokha, N.; Berns, H. Study on Nitrogen in Martensitic Stainless Steels. *HTM J. Heat Treat. Mater.* **2011**, *66*, 150–164. [[CrossRef](#)]
18. Burja, J.; Koležnik, M.; Župerl, Š.; Klančnik, G. Nitrogen and Nitride Non-Metallic Inclusions in Steel. *Mater. Tehmol.* **2019**, *53*, 919–928. [[CrossRef](#)]
19. Liverani, A.; Bacciaglia, A.; Nisini, E.; Ceruti, A. Conformal 3D Material Extrusion Additive Manufacturing for Large Moulds. *Appl. Sci.* **2023**, *13*, 1892. [[CrossRef](#)]
20. Habrman, M.; Chval, Z.; Ráž, K.; Kučerová, L.; Hůla, F. Injection Moulding into 3D-Printed Plastic Inserts Produced Using the Multi Jet Fusion Method. *Materials* **2023**, *16*, 4747. [[CrossRef](#)] [[PubMed](#)]
21. *ISO 6506-1:2014*; Brinell Hardness Test. Presentation and indication ISO Committee: Geneva, Switzerland, 2014.
22. *ISO 3685-1993 (E)*; Tool-Life Testing with Single-Point Turning Tools. Presentation and indication ISO Committee: Geneva, Switzerland, 1993.

Disclaimer/Publisher's Note: The statements, opinions and data contained in all publications are solely those of the individual author(s) and contributor(s) and not of MDPI and/or the editor(s). MDPI and/or the editor(s) disclaim responsibility for any injury to people or property resulting from any ideas, methods, instructions or products referred to in the content.